

Peak neutron production from the ${}^7\text{Li}(p,n)$ reaction in the 20-35 MeV range

Mitja Majerle^{1,*}, Alexander V. Prokofiev², Martin Ansorge¹, Pavel Bém¹, David Hladík¹, Jaromir Mrázek¹, Jan Novák¹, Eva Šimečková¹, and Milan Štefánek¹

¹Nuclear Physics Institute of the CAS, 250 68 Řež near Prague, Czech Republic

²Uppsala University, Division of Applied Nuclear Physics, Box 516, S-751 20, Uppsala, Sweden

Abstract. New experimental data on the peak neutron production in the ${}^7\text{Li}(p,n)$ reaction were collected during several irradiation campaigns at the NPI CAS. Time-of-flight method was used to measure the number of the peak neutrons in the forward direction, and the number of produced ${}^7\text{Be}$ nuclei was determined using γ -spectrometry. The new measurement results are compared with experimental data from the literature and used for the validation of several different systematics and nuclear data libraries developed over the years.

1 Introduction

Good knowledge of neutron cross sections is crucial in many fields of applied nuclear physics as well as for understanding of underlying fundamental physical processes. Neutron cross-section measurements are performed with a variety of neutron facilities [1], including monoenergetic ones below 20 MeV (making use of d+d, d+t reactions), quasi-monoenergetic above 20 MeV ($p+{}^7\text{Li}$, $p+\text{Be}$), as well as spallation neutron sources with thick targets and broad ("white") spectra.

Being an important source of quasi-monoenergetic neutrons (QMN) above 20 MeV, the ${}^7\text{Li}(p,n)$ reaction has been extensively studied during the past decades by many experimentalists and evaluators (see the quoted literature and references therein). The thickness of the Li target is usually chosen so that the energy losses for incident protons do not exceed a few MeV. Two contributions can then be discerned in the produced neutron spectrum in the forward direction (see examples in Fig. 1): high-energy peak neutrons (further referred to as "peak neutrons") due to the ${}^7\text{Li}(p,n){}^7\text{Be}(0+0.429\text{MeV})$ reaction, and continuum neutrons originating from other ${}^7\text{Li}(p,xn)$ reactions. A review and systematics of neutron spectra from the ${}^7\text{Li}(p,xn)$ reaction at 0° can be found in [2].

In the present paper we discuss the status of the knowledge of the peak neutron production in the ${}^7\text{Li}(p,n)$ reaction. Experimental data from several authors have been collected and compared with measurement results of the present work (further referred to as "the NPI CAS data"). Various theoretical models and empirical systematics based on the experimental data, developed over the years, are discussed and validated against the available measurement results.

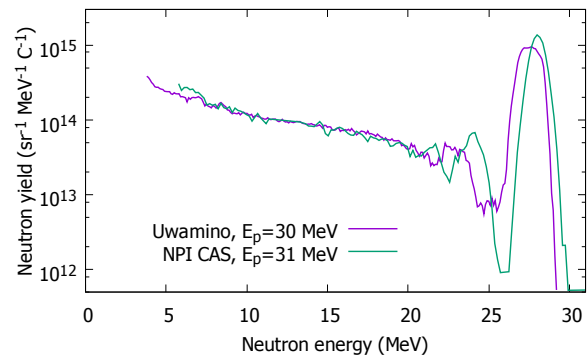


Figure 1. Experimentally measured neutron spectra from the ${}^7\text{Li}(p,n)$ reaction at 0° at the energy of the impinging protons 30 MeV [3] and 31 MeV (present work). The high-energy peak comprises the neutrons with the energy above 26 MeV, and the continuum lies below that energy.

2 Facility and methods

2.1 Neutron source

The QMN-generator at NPI CAS, based on the ${}^7\text{Li}(p,n)$ reaction, comprises a 2-mm thick lithium target (${}^7\text{Li}$ or ${}^{\text{nat}}\text{Li}$ metal) followed by a 1-cm thick carbon slab to stop protons that remain in the beam after passing the target. The target and the slab are electrically isolated to allow measurements of charge brought by impinging protons. The beam of protons, accelerated by the U-120M cyclotron and directed to the target, produces QMN (see an example of spectrum in Fig. 1). The proton energy can be set in the range 20-35 MeV. The design of the generator allows extraction of the lithium target after the irradiation (for γ -measurements). The cyclotron radio-frequency (RF) repetition period of 40-50 ns allows time-of-flight (TOF) measurements of the neutron spectra. Further details can be found in [4].

*e-mail: majerle@ujf.cas.cz

2.2 Peak neutron measurement methods

The peak neutrons are produced in the ${}^7\text{Li}(p,n)$ reactions that leave the resulting ${}^7\text{Be}$ nucleus in its ground state or in its first excited state. These two states are the only particle-emission-stable ones for that nucleus [5]. Therefore the number of peak neutrons emitted into the 4π solid angle during a given irradiation is equal to the number of produced ${}^7\text{Be}$ nuclei, which was accurately measured in the present work using the γ -spectrometry technique. Losses of ${}^7\text{Be}$ recoils out of the lithium target were estimated to be negligible.

Peak neutrons in the forward direction were detected with a $2''\times 2''$ liquid scintillator (NE213) in the TOF mode, at the distance 4-5 m. The scintillator was oriented with its axis along the proton beam direction. Signals from the scintillator and the RF were digitized simultaneously using the CAEN V1751 module (10 bit, 1 Gsample/s). Losses of signals due to acquisition dead-time and signal pile-up (up to a few %) were taken into account in the analysis. The charge comparison method was used to discriminate neutrons from γ -rays. The neutron TOF was obtained from the phase of the RF signal. For the calibration of the TOF scale we used the 4.438-MeV γ -peak produced by protons impinging on the carbon slab. The calibration of the response amplitude was performed using the Compton edge of those γ -rays (4.196 MeV), the double-escape peak, and the TOF-amplitude dependence of the neutron response.

Elastic scattering of neutrons on hydrogen nuclei in the scintillator determines the high-energy part of its response. Only that component was used in the analysis of the TOF spectra. Consequently, the peak-neutron detection efficiency of the scintillator (ϵ) was dependent only on the ${}^1\text{H}(n,p)$ elastic scattering cross section [6] and not dependent of cross sections of other neutron-induced reactions in the detector. That detection efficiency was determined in a simulation using the SCINFUL-R code [7], taking into account the properties of the scintillator: dimensions, distance to the Li target, as well as detector material composition and density. A sensitivity analysis of parameters of the TOF-measurement setup (the properties of the scintillator, its time resolution and amplitude calibration, as well as the elastic scattering cross section) was performed to determine their influence on the detection efficiency. The resulting systematic uncertainty in the efficiency amounted to 7-10% and dominated the uncertainty budget for the measurements, as reported in Table 1.

Differential cross section for production of forward-emitted neutrons was obtained from the measured number of peak neutrons $N_n(0^\circ)$:

$$(d\sigma/d\Omega)_{\theta=0} = \frac{N_n(0^\circ)}{\Omega_d \epsilon K_{\text{att}} N_p n_{\text{Li}-7}}, \quad (1)$$

where Ω_d is the solid angle of the scintillator, and K_{att} is a coefficient that characterizes attenuation of peak neutrons on their way to the detector. That coefficient was determined in simulations using the MCNPX 2.7.0 code [8]. Its deviation from unity ranges from 10 to 15%, decreasing in the studied range of peak-neutron energy (18-33 MeV). N_p stands for the number of protons impinging on the lithium target during the experiment. This quantity was deduced from the charge of protons collected by the isolated target

Table 1. The uncertainty budget in the NPI CAS measurements.

The source of uncertainty		The uncertainty in the determined quantity (%)		
Symbol	Uncertainty (%)	R	$\sigma({}^7\text{Be})$	$(d\sigma/d\Omega)_{\theta=0}$
$n_{\text{Li}-7}$	5	–	5	5
N_p	2	–	2	2
$N_{\text{Be}-7}$	2	2	2	–
ϵ	7-10	7-10	–	7-10
$N_n(0^\circ)$	<1	<1	–	<1
Ω_d	<1	<1	–	<1
K_{att}	<1	<1	–	<1
TOTAL		8-10	5-6	9-11

station. $n_{\text{Li}-7}$ is the number of ${}^7\text{Li}$ atoms in the target per unit area, calculated from target's thickness and density.

Uwamino [3] introduced an "index of forwardness" of the ${}^7\text{Li}(p,n)$ reaction:

$$R = \frac{(d\sigma/d\Omega)_{\theta=0}}{\int_{4\pi} (d\sigma/d\Omega) d\Omega}. \quad (2)$$

For the calculation of the denominator in Eq. 2, Uwamino integrated synthetic angular distributions of peak neutrons obtained by combination of experimental data [3, 5, 9] and Taddeucci's angular systematics [10] (for further details, see [3]). By fitting the obtained data points, Uwamino expressed the index of forwardness with the following empirical formula:

$$R (\text{sr}^{-1}) = -5.155 \cdot 10^{-13} E_p^4 + 4.409 \cdot 10^{-9} E_p^3 + 2.483 \cdot 10^{-5} E_p^2 + 6.521 \cdot 10^{-2} E_p - 0.8636, \quad (3)$$

where E_p is the incident proton energy (MeV). The declared uncertainty of the formula is 6%.

An alternative method, employed in the present work for determinations of the factor R , makes use of the production of ${}^7\text{Be}$ nuclei in the Li target, as a measure of the total production of peak neutrons. The index of forwardness can then be calculated as:

$$R = \frac{(d\sigma/d\Omega)_{\theta=0}}{\sigma({}^7\text{Be})}, \quad (4)$$

where $\sigma({}^7\text{Be})$ is the cross section of the ${}^7\text{Li}(p,n){}^7\text{Be}$ reaction:

$$\sigma({}^7\text{Be}) = \frac{N_{\text{Be}-7}}{n_{\text{Li}-7} N_p}, \quad (5)$$

where $N_{\text{Be}-7}$ is the number of produced ${}^7\text{Be}$ nuclei, determined using the γ -spectroscopy technique.

In the present work, both the quantities $(d\sigma/d\Omega)_{\theta=0}$ and $\sigma({}^7\text{Be})$ have been determined in the same beam exposures. The determinations of $\sigma({}^7\text{Be})$ are described in the recent paper [4]. The R -factor data were obtained in the same beam exposures without involving the quantities $n_{\text{Li}-7}$ and N_p . Indeed, combining Eqs. 1, 4, and 5, we arrive at a simplified equation for the experimental determination of the R -factor:

$$R = \frac{N_n(0^\circ)}{\Omega_d \epsilon K_{\text{att}} N_{\text{Be}-7}}. \quad (6)$$

The overall uncertainty in the R -factor is therefore reduced to the uncertainties in the neutron detection efficiency (7-10%) and in the γ -spectrometry measurement (2%).

Table 2. The experimentally measured NPI CAS data. The quoted energy is the average proton energy in 2-mm thick lithium target. The energy settings marked with * were used with ^{nat}Li targets, see the main text for further details. The result marked with ** was obtained using a proton-recoil telescope [11].

Energy (MeV)	R (sr^{-1})	$\sigma(^7\text{Be})$ (mb)	$(d\sigma/d\Omega)_{\theta=0}$ (mb/sr)	Year/month
19.1±1.2*	0.50±0.05			17/2
21.3±1.1*	0.66±0.07			17/4
21.4±1.1	0.49±0.04	31.9±1.8	17.0±1.5	14/3
23.7±1.0*	0.66±0.07			17/10
24.1±1.0	0.78±0.06	29.4±1.6	22.6±2.2	14/2
26.6±0.9			26.7±2.4	13/3
26.7±0.9*	0.69±0.07			18/2
26.7±0.9**			25.0±2.5	10/1
26.8±0.9*	1.03±0.11			16/1
29.2±0.9*	1.01±0.10			16/5
29.6±0.8	1.18±0.12	22.2±1.1	26.3±3.0	13/5
31.5±0.8*	1.65±0.17			17/1
31.6±0.8*	1.49±0.15			18/11
31.7±0.8	1.48±0.12	18.3±0.9	26.8±2.6	13/9
34.3±0.7	1.48±0.15	18.8±0.9	30.5±3.5	13/10
34.4±0.7*	1.26±0.13			17/9

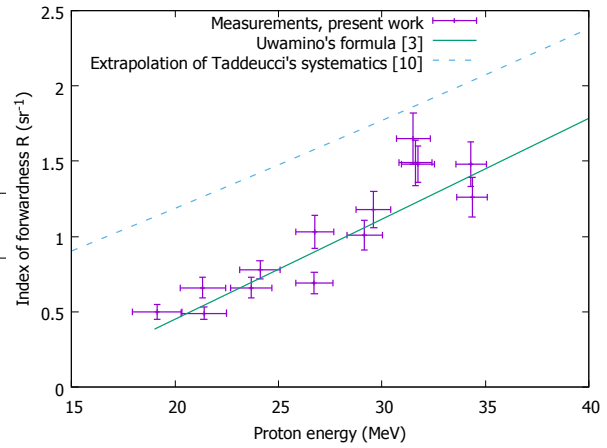


Figure 2. The index of forwardness in the $^7\text{Li}(p,n)^7\text{Be}$ reaction versus proton energy. (Here and further in the paper, we use the term "proton energy" for the average energy of protons in the Li target). The experimental data obtained in the present work are shown by symbols. Predictions of Uwamino's formula (see Eq. 3 and [3]) are represented by the green solid line. An extrapolation of Taddeucci's angular systematics [10] is shown by the dashed blue line (see the main text for further details).

3 Results and discussion

In Table 2, the data of the present work are given for all three measured quantities: $\sigma(^7\text{Be})$, $(d\sigma/d\Omega)_{\theta=0}$, and the R -factor, versus proton energy. The data for $\sigma(^7\text{Be})$ have been earlier reported in [4] and in the EXFOR entry D0910003. The energy settings marked with an asterisk in Table 2 were used with ^{nat}Li targets with poorly known content of ^7Li . In those cases, only the factor R was measured, whereas the absolute values of $\sigma(^7\text{Be})$ and $(d\sigma/d\Omega)_{\theta=0}$ could not be determined. More detailed presentation and discussion of the results is given in Sect. 3.1-3.3.

3.1 The index of forwardness (the R -factor)

The obtained R -factor data, given in Table 2, are also shown in Fig. 2 together with predictions of Uwamino's formula [3]. Taddeucci [10] proposed empirical systematics of angular distributions of peak neutrons in the studied reaction in the range of 80-800 MeV. In Fig. 2 we show the energy dependence of the R -factor calculated using an extrapolation of the systematics [10] towards lower proton energies. As seen in the figure, the extrapolation reproduces correctly the trend in the studied energy dependence, whereas it overestimates the absolute index-of-forwardness data by a factor of 1.5-2 in the energy range of 20-35 MeV.

3.2 The $^7\text{Li}(p,n)^7\text{Be}$ cross section

The data for the $\sigma(^7\text{Be})$ cross section, measured in our recent work [4] with the experimental setup presented above, are given in Table 2 and shown in Fig. 3 in comparison with the results of other authors [5, 12-14]. Taddeucci [10] proposed an empirical fit for $\sigma(^7\text{Be})$ (mb):

$$\ln(\sigma(^7\text{Be})) = a + b \cdot \ln(E_p), \quad (7)$$

where $a = 7.02 \pm 0.05$ and $b = -1.13 \pm 0.01$. A part of the fitting curve, obtained in the energy range 25-480 MeV, is also shown in Fig. 3.

As seen in Fig. 3, the data sets of Refs. [4], [13], and [5] disagree beyond their uncertainty limits. The disagreement, up to 8%, may directly impact other cross sections measured with $^7\text{Li}(p,n)$ neutron sources. In the 25-35 MeV range, the Taddeucci's empirical fit [10] seems to overestimate the experimental data of Refs. [4, 12, 13] by $\approx 10\%$. On the other hand, this deviation is comparable to the spread of the experimental data points as well as to the uncertainty in the fit [10] itself.

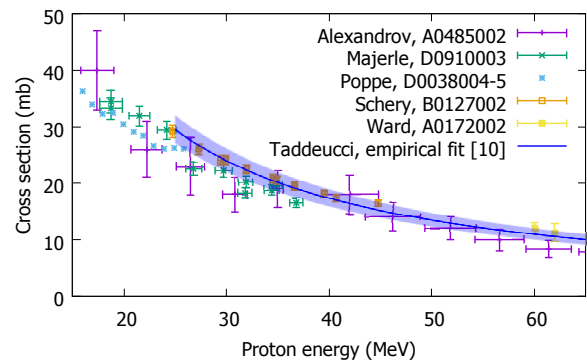


Figure 3. Total cross sections of the $^7\text{Li}(p,n)^7\text{Be}$ reaction. The experimental data [4, 5, 12-14] are represented by symbols. EXFOR ID numbers are given for each data set. The uncertainties of the data of Poppe [13], obtained by integration of the angular cross sections, have been estimated to 10%. The global empirical fit proposed by Taddeucci [10] is shown by a line, with a corridor of uncertainty reflecting the uncertainties in the fitting parameters quoted in [10].

3.3 The forward-emitted peak neutrons

The differential cross sections of peak-neutron production in the ${}^7\text{Li}(p,n)$ reaction at 0° , measured in the present work, are given in Table 2 and shown in Fig. 4 in comparison with abundant experimental data from other studies [5, 9, 10, 13, 15–20]. The NPI CAS values are in good agreement with the experimental data of Poppe [13] below 25 MeV.

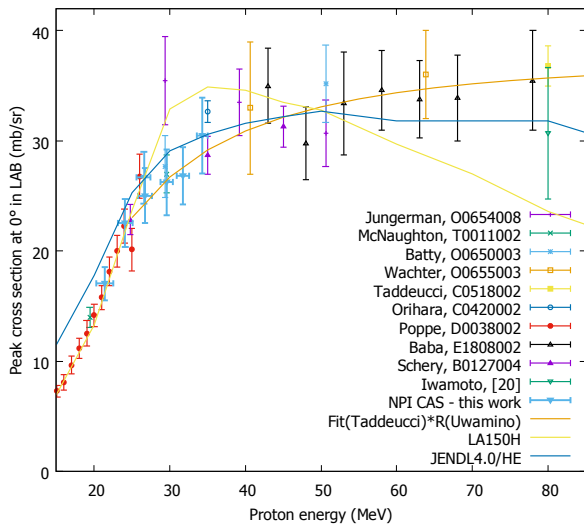


Figure 4. The differential cross section for neutron production in the ${}^7\text{Li}(p,n){}^7\text{Be}$ reaction at 0° . The experimental data [5, 9, 10, 13, 15–20] are represented by symbols. EXFOR ID numbers are given for each data set. The lines represent the combination of the systematics [10] and [3] (brown-colored line) as well as the predictions of the LA150H and JENDL4.0/HE libraries (yellow- and blue-colored lines, respectively).

The brown-colored line in Fig. 4 represents a function obtained by combining the Uwamino’s formula [3] with the Taddeucci’s empirical fit for the $\sigma({}^7\text{Be})$ cross section [10]. The resulting function agrees well with the experimental data above 30 MeV [5, 10, 15, 17–20], whereas at lower energies the agreement is worse. This deviation reflects the disagreements between Eq. 7 and the experimental data as shown in Fig. 3.

Data for the cross section $(d\sigma/d\Omega)_{\theta=0}$ were retrieved from two evaluated data libraries for the ${}^7\text{Li}(p,n)$ reaction: LA150H [21] and JENDL4.0/HE [22]. The results are also shown in Fig. 4. As seen in the figure, none of the libraries is capable of reproducing the available experimental data in the entire considered energy range, 15–80 MeV. On the other hand, the LA150H library reproduces the data very well at low energies up to ≈ 25 MeV. Above that energy, the best representation of the data is still given by a combination of the empirical systematics [10] and [3].

4 Conclusions and outlook

New experimental data on the peak neutron production in the ${}^7\text{Li}(p,n)$ reaction have been measured. They agree reasonably with other experimental results and fill a gap in the range not covered by existing data.

Empirical formulas by Taddeucci (for the peak-neutron production cross section) and by Uwamino (for the index of forwardness, R) have been validated against all available experimental data in the studied energy range. It has been found that Taddeucci’s empirical formula reproduces well the experimental data above 35 MeV. Below 35 MeV, there are disagreements between measured data sets by different authors. A dedicated stacked-foil experiment is planned at the NPI CAS to determine the cross section with lower uncertainty.

Two evaluated data libraries for the ${}^7\text{Li}(p,n)$ reaction are in use nowadays: LA150H and JENDL4.0/HE. The tabulated values of production cross sections for forward-emitted peak neutrons have been compared with experimental data and disagreements have been revealed. This work demonstrates that renormalization of simulated spectra to expert-evaluated experimental results may often be necessary.

Acknowledgments

The measurements were carried out at the infrastructure CANAM of the NPI CAS Řež, supported by the Ministry of Education, Youth and Sports of the Czech Republic under the project EF16_013/0001812.

References

- [1] *Compendium of Neutron Beam Facilities for High Precision Nuclear Data Measurements*, Number 1743 in TECDOC Series (IAEA, Vienna, 2014), ISBN 978-92-0-106614-5
- [2] A.V. Prokofiev et al., *J Nucl Sci Technol* **39**, Suppl. 2, 112 (2002)
- [3] Y. Uwamino et al., *NIM A* **389**, 463 (1997)
- [4] M. Majerle et al., *Nucl Phys A* **953**, 139 (2016)
- [5] S.D. Schery et al., *NIM* **147**, 399 (1977)
- [6] O. Cabellos, *Nuclear Data Sheets* **118**, 456 (2014)
- [7] S. Meigo, *NIM A* **401**, 365 (1997)
- [8] D. B. Pelowitz, Tech. Rep. LA-CP-11-00438, Los Alamos National Laboratory (2011)
- [9] H. Orihara et al., *NIM A* **257**, 189 (1987)
- [10] T.N. Taddeucci et al., *Phys Rev C* **41**, 2548 (1990)
- [11] J. Novák et al., *J Korean Phys Soc* **59**, 1577 (2011)
- [12] V.N. Aleksandrov et al., *Vopr Atomn Nauki i Tekhn, Ser Yad Fiz Issledo* (8/16), 17 (1990)
- [13] C.H. Poppe et al., *Phys Rev C* **14**, 438 (1976)
- [14] T.E. Ward et al., *Phys Rev C* **25**, 762 (1982)
- [15] J.A. Jungerman et al., *NIM* **94**, 421 (1971)
- [16] M.W. McNaughton et al., *NIM* **130**, 555 (1975)
- [17] C.J. Batty et al., *NIM* **68**, 273 (1969)
- [18] J.W. Wachter et al., *NIM* **113**, 185 (1973)
- [19] M. Baba et al., *NIM A* **428**, 454 (1999)
- [20] Y. Iwamoto et al., *NIM A* **804**, 50 (2015)
- [21] S.G. Mashnik et al., Report LA-UR_00-1067, Los Alamos (2000)
- [22] S. Kunieda et al., *IAEA-Conf* **004**, 41 (2016)